BNL-65190

Soft X-Ray Circular Dichroism and Scattering Using a Modulated, Elliptically Polarizing Wiggler and Double Synchronous Detection

John C. Sutherland,[†] Krzysztof Polewski,[†] Denise C. Monteleone,[†] John G. Trunk,[†] Gary A. Nintzel,[‡] Dennis G. Carlson,[‡] Qing-Li Dong,[‡] Om V. Singh,[‡] Steven L. Hulbert,[‡] Chi-Chang Kao,[‡] and Erik D. Johnson[‡]

Biology Department[†] and National Synchrotron Light Source,[‡] Brookhaven National Laboratory, Upton, NY 11973-5000 USA

CONF-980117--

ABSTRACT

We have constructed an experimental station (beamline) at the National Synchrotron Light Source to measure circular dichroism (CD) using soft x-rays ($250 \le h\nu \le 900$ eV) from a time modulated elliptically polarizing wiggler. The polarization of the soft x-ray beam switches periodically between two opposite polarizations, hence permitting the use of phase-sensitive (lock-in) detection. While the wiggler can be modulated at frequencies up to 100 Hz, switching transients limit the actual practical frequency to ≈ 25 Hz. With analog detection, switching transients are blocked by a chopper synchronized to the frequency and phase of the wiggler. The CD is obtained from the ratio of the signal recovered at the frequency of polarization modulation, f, to the average beam intensity, which is recovered by synchronous detection at frequency $2f$.

Keywords: Circular dichroism, x-rays, synchrotron radiation, synchronous detection

1. INTRODUCTION

Circular dichroism, the difference in the absorption of left and right circularly polarized electromagnetic radiation, is one of several manifestations of optical activity. The underlying mechanism can be either inherent or induced asymmetry of the absorbing species. Circular dichroism has been an important tool for studies of chemical and biochemical systems since the invention of sensitive scanning ellipsometers by Grosjean and Legrand[1] nearly 40 years ago. Their use of phase-sensitive detection, made possible by what is now known as a "lock–in" amplifier, was responsible for the increase in sensitivity achieved by their instrument, which resulted in the subsequent surge in interest in chiral methods. The second major improvement in circular dichroism instrumentation occurred a decade later when photoelastic modulators replaced Pockels cells as the means of converting a beam of linearly polarized light into a beam that alternates between left and right circularly polarized.[2-4] Because photoelastic modulators, unlike Pockels cells, can be fabricated from a wide variety of optical materials, they led to a huge increase in the spectral range accessible to circular dichroism spectroscopy in both the infrared[5] and ultraviolet.[6] However, photoelastic modulators require a transparent, compressible optical material, and hence are not practical for photon energies greater than about 10 eV ($\lambda < 120$ nm).

Accelerator-based radiation sources, such as synchrotron storage rings and free electron lasers, can be configured to produce circularly or elliptically polarized radiation over a huge range of photon energies. There is little need for such approaches at photon energies less than 10 eV, where photoelastic modulators are available, (although, between roughly 6 and 10 eV synchrotron sources used in conjunction with photoelastic modulators offer excellent performance[6]). At higher energies, however, synchrotrons and free electron lasers offer the main

avenue to extending circular dichroism spectroscopy. There are two approaches to generating circularly or elliptically polarized radiation from synchrotrons or free-electron lasers. (For a recent review see Sutherland[6]). First, linearly polarized radiation, which is the "default" output mode for most Accelerator-based sources, can be converted into circularly or elliptically polarized light either by transmission through an appropriate crystal, or by a series of reflections. Transmission is best for hard x-rays and reflection is appropriate for soft x-rays. While the notion of alternating a beam of linearly polarized radiation is conceptually similar to the strategies used at lower photon energies, reversal of the handedness of the radiation requires some sort of mechanical manipulation of the modulator. Such manipulations inside an ultrahigh vacuum system are possible, albeit nontrivial, but avoiding spurious modulations of intensity or degree of polarization and achieving reasonable throughput may be significant challenges. One advantage of such approaches is that the polarization specific components are deployed outside of the storage ring or free-electron laser, thus increasing flexibility and decreasing cost.

The second approach is to either manipulate or view the electron beam in a manner that results directly in a circularly or elliptically polarized radiation. As electrons sweep through a uniform magnetic field, the radiation emitted tangentially to their orbits is linearly polarized in the orbital plane, but becomes progressively more elliptically polarized as the viewing angle moves out of that (usually horizontal) plane, and the handedness above the orbital plane is opposite that beneath this plane. The degree of circular polarization increases monotonically as the viewing angle moves away from the orbital plane, but, alas, the intensity decreases monotonically at the same time, with complete circular polarization achieved just as the intensity vanishes. These transitions in ellipticity occur over an angular range of a few milliradians. Such "over-and-under" methods are applicable only for bending magnets, in which an electron (or positron) beam traverses a single magnetic field. Such methods cannot be used with "wigglers" (arrays of magnets that alternate in field direction and which are located in straight sections of storage rings between bending magnets) because the sign of the ellipticity alternates with each change in field direction. The first experiments that used elliptically polarized synchrotron radiation from the bending magnets of a storage ring were designed so that only light emitted above or below the orbital plane reached the sample.[7,8] While this arrangement is adequate for experiments that require steady elliptically polarized light, attempts to perform modulated experiments in which photon beams taken from opposite sides of the orbital plane are alternately directed to the sample are limited by difficulties in matching optical throughputs. For example, certain metallo-proteins with degenerate ground states exhibit very large magnetic circular dichroism signals at temperatures near absolute zero, both in the visible [9,10]and x-ray regions.[11] Most organic and biologically important molecules, however, exhibit only weak natural circular dichroism in the ultraviolet, visible and infrared,[12] and theoretical calculations suggest that the same situation will prevail for x-rays as well.[13]

Many approaches have been proposed to permit periodic reversal of the helicity of x-rays beams while maintaining a constant optical path. Of interest here is the notion of tipping the pitch of the electron beam as it passes through a magnetic field so that an observer viewing the electrons from a position exactly in the plane of the (unperturbed) orbit will view either the top or bottom of the instantaneous orbit. For a given direction of bending by a main (vertically oriented) magnet, reversing the pitch deviation from the horizontal thus reverses the observed helicity. [14-16] This is the approach used in the system described herein.

DISCLAIMER

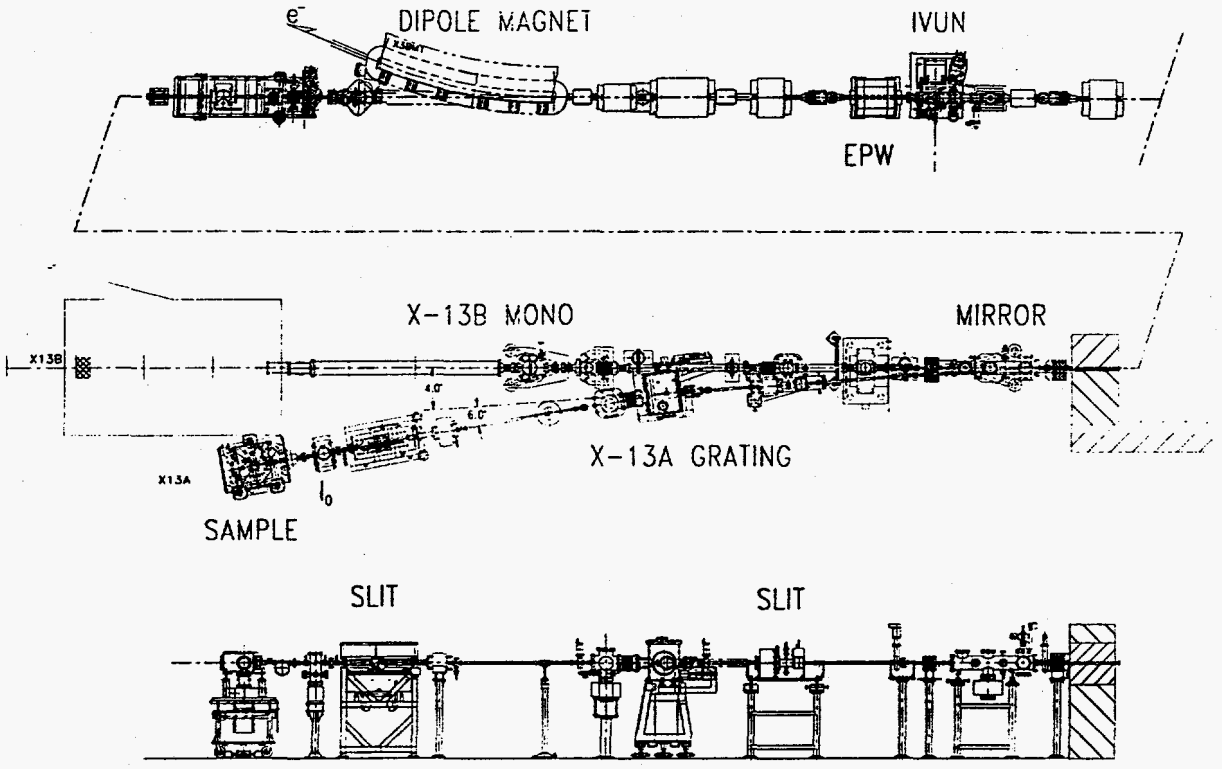

Figure 1 Diagram of beamline X13 at the NSLS. The top panel shows the straight section of the storage ring that the Elliptically Polarizing Wiggler (EPW) shares with another insertion device (an In-Vacuum Undulator, IVUN). The beam of electrons circulating within the storage ring enters this section from the right of the figure. The photon beam generated by either the EPW or the IVUN exits the storage ring vacuum chamber at a port located within the field produced by a dipole magnet that separates the electron beam circulating in the storage ring from the photon beam, which is traveling to the left in the figure. The vacuum chamber containing the photon beam passes through a series of shutters and valves and then through a radiation shield wall, which is the first element shown on the right-hand side of the center and lower panels. The center panel is a plan view of beamline X13 outside of the shield wall. A mirror located just outside the shield wall deflects the beam through 4° and focuses it on the entrance slit of the monochromator of X13A, the soft x-ray beamline described here. This mirror can be withdrawn to allow the beam to pass into beamline X13B, which is configured for experiments using higher energy x-rays. The experimental apparatus for X13B is contained within a radiation area exclusion structure (hutch) shown only as a rectangular outline. The lower panel is an elevation view showing only those components specific to X13A or common to both branches. The major components of X13A are, from right to left, the entrance slit, grating monochromator, exit slit, and sample chamber. A hutch is not required to contain the soft-x-rays reaching the X13A sample chamber. The electronics, computer system, and operator console are located to the left of the sample chamber.

2. SOFT X-RAY BEAMLINE

The elliptically polarizing wiggler is presently installed in a straight section that delivers photons to beamline X13 at the National Synchrotron Light Source. This wiggler supplies x-rays to either the soft-x-ray beamline described here (X13A) or to an adjacent, downstream beamline (X13B) that is optimized for higher energy photons as shown in Figure 1. The distance from the center of the straight section of the storage ring containing the wiggler to the end of the beamline is approximately 26 m. All optical components are mounted within UHV compatible vacuum chambers.

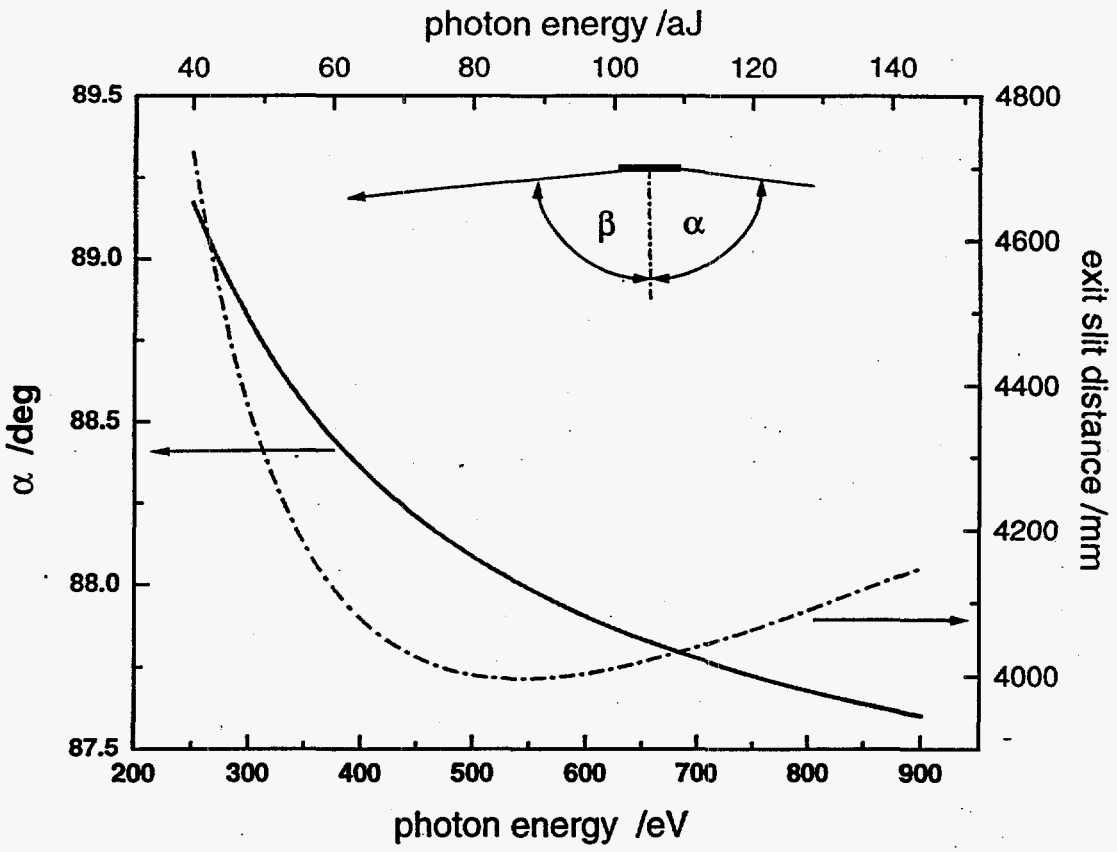

Figure 2 The angle of incidence, α, between the incident x-ray beam and the grating normal (left axis, ——) and the distance from the grating to the exit slit (right axis, - - - -) as a function of photon energy. The monochromator is tuned to select a particular photon energy from the incident beam of synchrotron radiation by moving the grating and exit slit to the locations corresponding to the positions shown above. These locations are represented directly as a number of steps generated by a stepping motor from a reference location. In this configuration, the exit angle, β, is given as a negative number by convention because the incident and exit axes of the monochromator are on opposite sides of the grating normal.[17] Thus, α and β are related by the equation $\alpha - \beta = 174°$.

2.1 Modulated Elliptically Polarizing Wiggler

The elliptically polarizing wiggler, which has been described previously,[16] consists of five 0.8 T permanent main magnets plus two 0.4 T end magnets all aligned in the vertical plane with alternating field directions. In addition, there are a total of 10 variable field electromagnets with alternating field directions oriented in the horizontal plane. These magnets control the pitch of the electron beam as it traverses the wiggler. The synchrotron radiation that reaches the sample is produced as the electron beam is deflected in the horizontal plane by the alternating vertically directed magnetic fields of the array of permanent magnets. If the electromagnets are not energized, the x-rays produced by the wiggler are linearly polarized with their electric vectors in the horizontal plane. The effect of the electromagnets is to alternately tip the beam so that it is directed slightly upwards as it passes through the field of one of the permanent magnets and slightly downwards as it passes through the field of the next permanent magnet. For a given polarity of the main vertically directed magnetic fields, the radiation emitted above the plane of the orbit will be elliptically polarized to the same degree, but with the opposite polarity, as the radiation emitted at the same angle but on the opposite side of the orbital plane.[18] The effect of tipping the electron beam slightly up or down is to cause elliptically, rather than linearly, polarized radiation to be emitted in the horizontal plane and hence travel through the beamline to the monochromator and sample. The combined effect of the alternating directions of both the main vertical-field electromagnets is thus to change both the direction of curvature and the direction of out-of-plane tilting for each successive main magnet, with the result that all of the emerging x-rays are elliptically polarized with the same handedness. Reversing the polarities of the electromagnets *en mass* reverses the handedness of the output beam, but great care is required in adjusting the currents that energize the electromagnets to ensure that only the sign and not the intensities and degree of helicity of the beam are altered. In addition, the weaker electromagnets on the ends of the array must be adjusted to prevent these perturbations of the orbit of the circulating electron beam within the wiggler from modulating the motion of the electron beam at remote locations around the storage ring, which would interfere with experiments on other beamlines. The electromagnets were designed so that the polarity of the helicity can be reversed at up to 100 Hz, however, switching transients limit the actual upper frequency to a lower value (see below).

2.2 Monochromator

Soft x-rays are selected from the broad spectrum produced by the wiggler by a near grazing-incidence, UHV, spherical grating monochromator constructed by Oxford Instruments Accelerator Technology Group (Oxford, Oxon, UK). Dispersion is in the horizontal plane, which is atypical for monochromators employed with synchrotron radiation sources. The X-13 monochromator can be fitted with two gratings that can be interchanged *in situ*. The grating presently in use is ruled at 800 lines/mm and has a radius of curvature of 57.3 m. A fixed entrance slit is located 2.0 m from the axis of rotation of the grating. The exit axis of the monochromator is displaced by 6° with respect to its entrance axis. Wavelength selection is achieved by rotation of the grating about a vertical axis. That is, for zero-order, the angle of incidence and the angle of reflection are both equal to 87°. For the 800 l/mm diffraction grating, operating in first (inside) order, the 250 to 900 eV spectral range corresponds to grating angles of incidence that vary from 87.6 to 89.2 degrees. An 1800 l/mm grating will cover the spectral range from 600 to 1,800 eV. For a fixed position of the entrance slit, the location of the focus along the fixed exit axis is a function of photon energy. Thus, the exit slit, which was built by McPherson Instruments (Acton, MA), is mounted on a translator with vacuum continuity

maintained by UHV bellows. The exit slit can be moved up to 500 mm along the exit axis, with the center of this range located about 4.25 m from the grating axis. The monochromator is configured for each desired photon energy by coordinated rotations of the grating and translation of the exit slit. Neither location is a linear function of photon energy as shown in Figure 2. The grating and exit slit motions are not linked mechanically. Both the grating and the exit slit are moved by stepping motors under computer control as shown schematically in Figure 3.

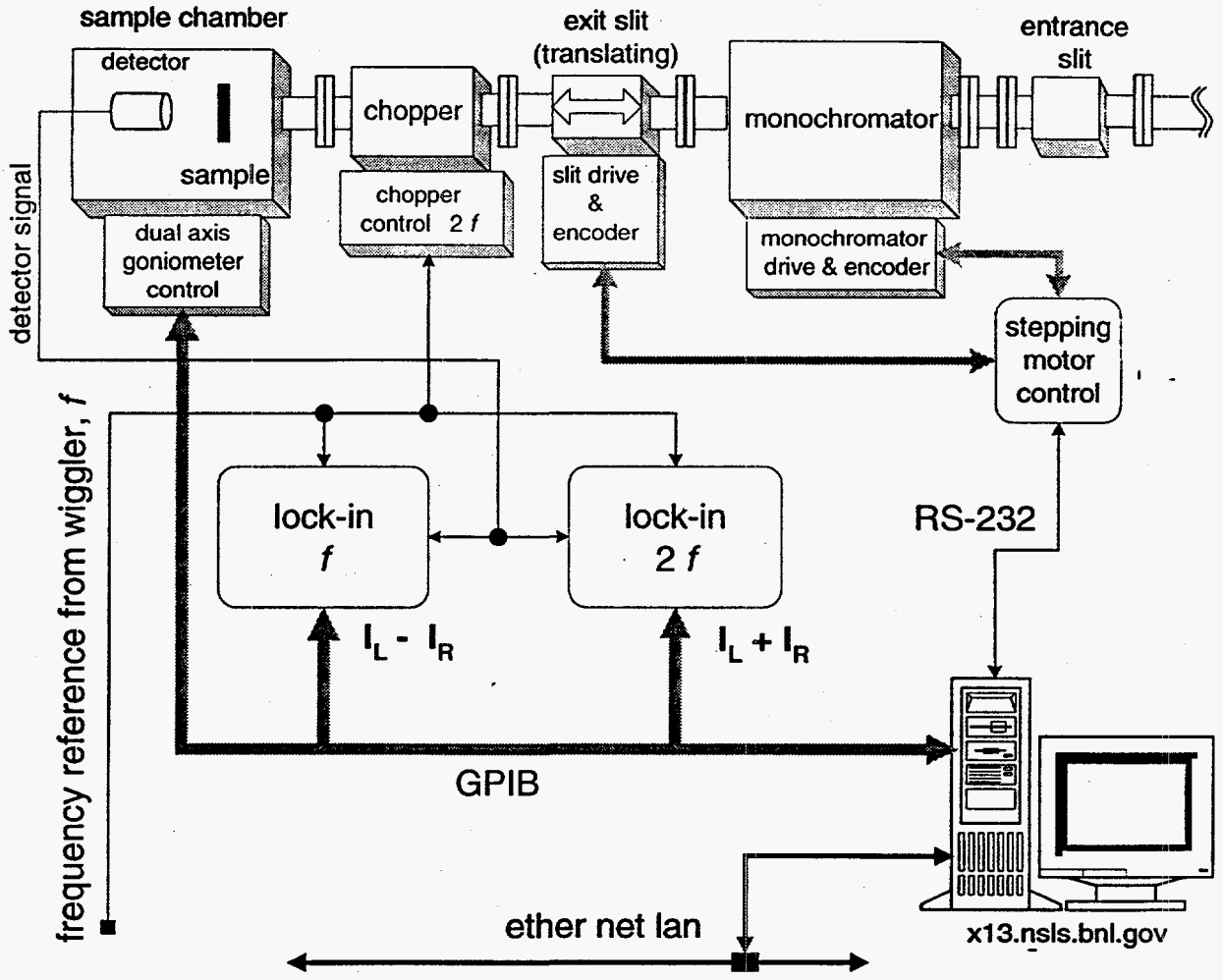

Figure 3 Schematic diagram of the beamline from the monochromator entrance slit to the sample chamber, electronics, and computer system that controls the operation of the beamline and acquires experimental data. Not to scale. The sample chamber is shown in greater detail in Figure 6. The computer controls the rotation of the grating and translation of the exit slit and determines their status from the associated encoders *via* an RS-232 serial link to a stepping motor control circuit supplied with the monochromator. After conditioning, signals from the detector are applied to the analog input channels of two lock-in amplifiers. An analog signal that indicates the frequency and phase of the wiggler polarization is applied to the reference inputs of both lock-ins and also to the rotating chopper. One lock-in is tuned to the frequency, f, of the elliptically polarizing wiggler, while the second lock-in and the chopper are tuned to 2f.

2.3 Beam Chopper

The intensity of the synchrotron beam reaching the sample is greatest when the electron beam is not deflected from the unperturbed orbital plane. Thus, every switch in helicity is accompanied by a transient spike in intensity. Following such a switch, there is a brief period in which the intensity is unstable as the beam settles into its new trajectory. These effects are shown schematically in Figure 4. When the signal from the sample is obtained by counting of individual photons, the effects of these transient signals can be avoided by gating of the counters that record the signal pulses using established methods.[19] The detection of small anisotropies requires acquisition of signal levels that exceed the practical limits of photon counting methods, and are better adapted to analog signal detection.

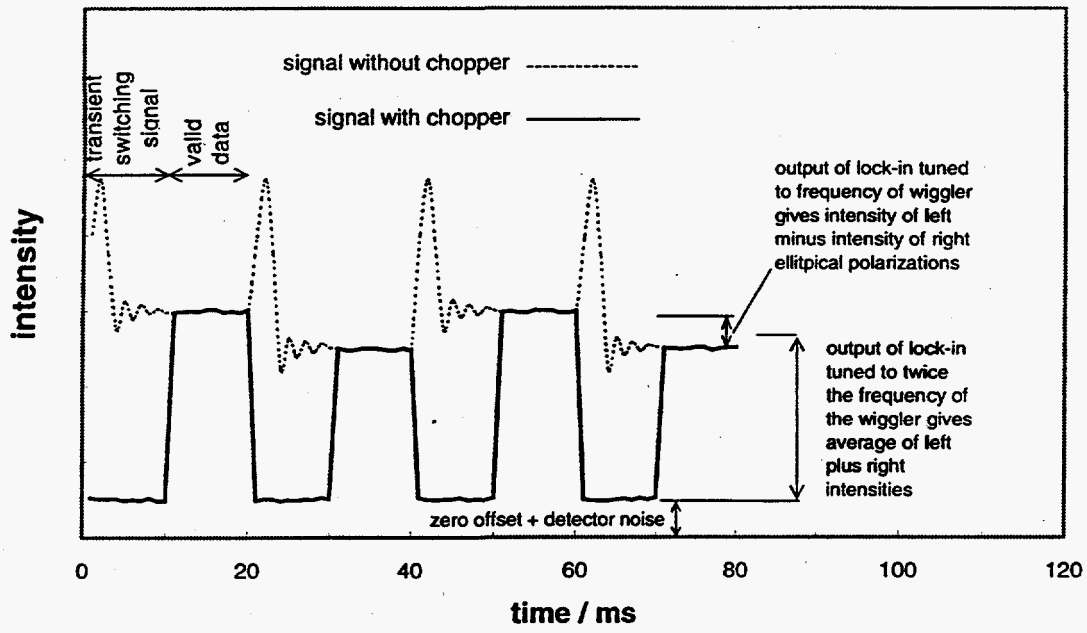

Figure 4 Schematic diagram showing the waveform generated by the beam from the elliptically polarizing wiggler that has been amplitude modulated by a sample that exhibits circular dichroism. The wiggler is shown operating at a frequency of 25 Hz, and hence a period of 40 ms. During each cycle, the polarization shifts from left to right and back to left, so there are two transient spikes per period; the first for the left-to-right transition and the second for the right-to-left transition. The transition spike is followed by a period of instability while the beams "settles." Circular dichroism is the difference between the absorption of left- and right-circularly polarized light. It is found by dividing the difference in intensity (for the stable data) for the two polarization states by their average value. The differences in intensity for the two polarization states shown in this figure are greatly exaggerated compared to the differences that are detectable using our new "lock-in" method.

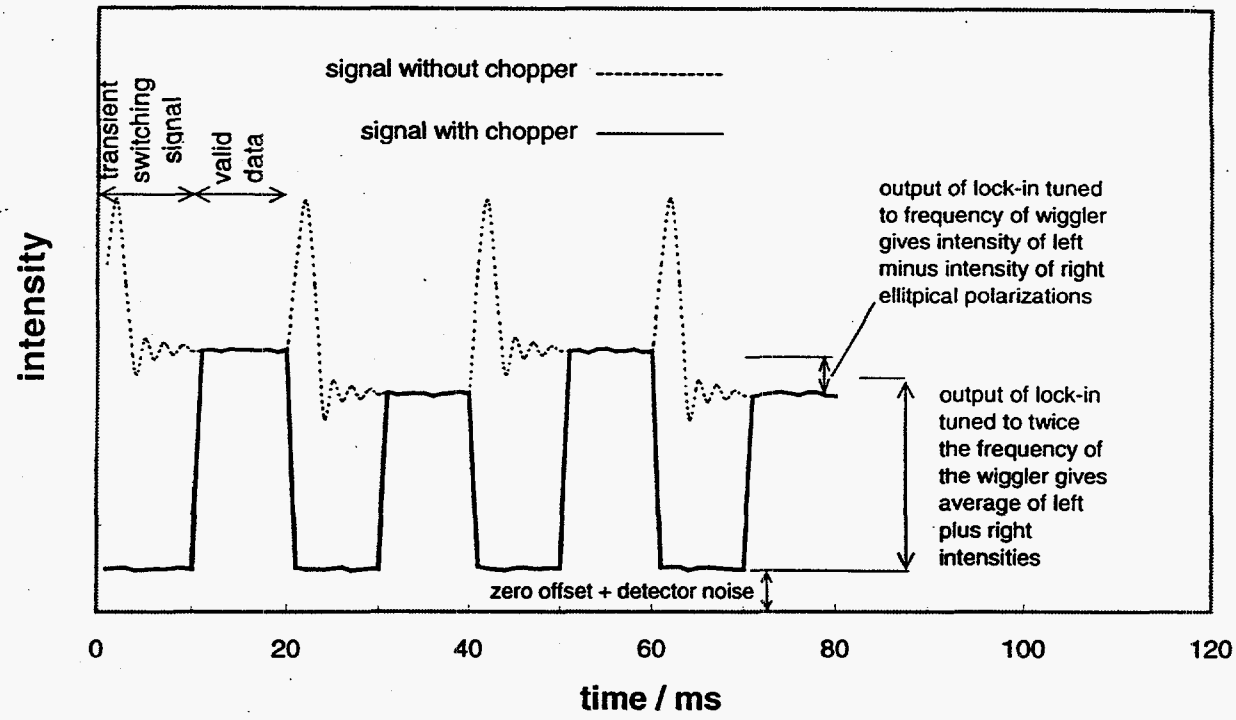

Figure 5 The waveform of the beam from the elliptically polarizing wiggler modulated by circular dichroism showing the effect of the beam "chopper" blocking the switching transients. The frequency of the open-closed cycle of the chopper is twice that of the wiggler. In our new method for detecting x-ray circular dichroism, a lock-in amplifier tuned to the frequency of the wiggler produces a signal proportional to the difference in intensity of the left- and right-intensities, while a second lock-in amplifier tuned to the frequency of the chopper (*i.e.*, twice the frequency of the wiggler) gives a signal proportional to the average value of the left- and right-intensities. The circular dichroism is the negative of the ratio of these signals. Note that the output of the *2f* lock-in automatically corrects for any zero-offset or "dark signal," which is not the case when the selection of the polarization signals is done with simple, two channel digital gating.

We prevent the switching transients from reaching the detector, and hence interfering with the extraction of the signal, by "chopping the photon beam at a frequency twice that of the switching frequency of the wiggler, as shown schematically Figure 5. For this purpose, we use a rotating sector chopper (model 3501, New Focus Inc., Santa Clara, CA) that can be slaved to the phase and the second harmonic of the frequency of the wiggler. The standard sector wheel was replaced with a 1.5 mm thick wheel (Bromac Inc., Palo Alto, CA) to insure complete attenuation of the x-ray beam. The chopper is installed in a separate vacuum housing located between the exit slit and the sample chamber, and is separated from the other spaces by aluminum windows.

2.4 Incident Intensity Monitor

The incident intensity of the beam can be monitored with a metal mesh detector located before or immediately after the chopper housing, and hence operated in a transmission mode. While not required for the measurement of circular dichroism, a measure of the intensity of the incident radiation is used in concomitant recording of the absorption of samples, and is also a useful diagnostic tool. This component and its associated electronics are not shown in Figure 3. The signal from the metal mesh monitor is acquired in digital form *via* one of the auxiliary A/D inputs of the lock-in amplifiers.

2.5 Sample and Detector Chamber

The last component of the beamline is a vacuum chamber that houses both the sample and the detector. A schematic diagram of this chamber is shown in Figure 6. The sample is mounted on a mount that can be rotated through an angle of 2π while the detector is mounted on the end of an arm that can be rotated through an angle that exceeds $\pi/2$. The angular orientations of sample and detector are controlled independently by a two circle goniometer (Picker X-ray Corp., Cleveland, OH) driven by stepping motors that operate under computer control. A variety of detectors can be accommodated, including photodiodes, gas proportional counters, or Ge and Si drift detectors (that would be used for fluorescence detection).

The monochromator/exit slit and sample chamber can be operated in four modes defined by the program controlling data acqusition:

In a **Photon Energy Scan** the angular positions of the sample and detector are fixed and the monochromator grating and exit slit are moved to select a series of (equally spaced) photon energies. The detector can be positioned at any angle within its range, as shown in Figure 6, including the "inline" orientation so that it intercepts the transmitted x-ray beam, as well as other angles where it will record scattered photons. Fluorescence can be monitored by introducing an appropriate detector through the port located adjacent to the sample position on the axis perpendicular to the incident beam.

A **Detector Angle Scan** is used to determine the scattering pattern produced by a sample at a fixed orientation and photon energy. Thus θ and photon energy remain fixed, while ϕ is scanned in uniform steps.

A **Sample Orientation Angle Scan** measures the scattering patterns observed for a fixed photon energy and detector angle; θ is scanned in uniform increments through a predetermined range.

A **Constant Angular Deviation Scan** involves rotation of both the sample and the detector such that the $\phi = 2\theta + \delta$. A **Specular Reflection Scan** is the special case for which $\delta = 0$.

2.6 Measurement of Circular Dichroism and Absorption

Circular dichroism is the difference in the absorption of left and right circularly polarized radiation. Because the attenuation of a photon beam is a statistical process in which the rate of loss is proportional to the remaining intensity, we can represent the intensity of a beam of radiation of wavelength λ and initial intensity I_0 that has penetrated a distance x into a material of thickness d by the equation

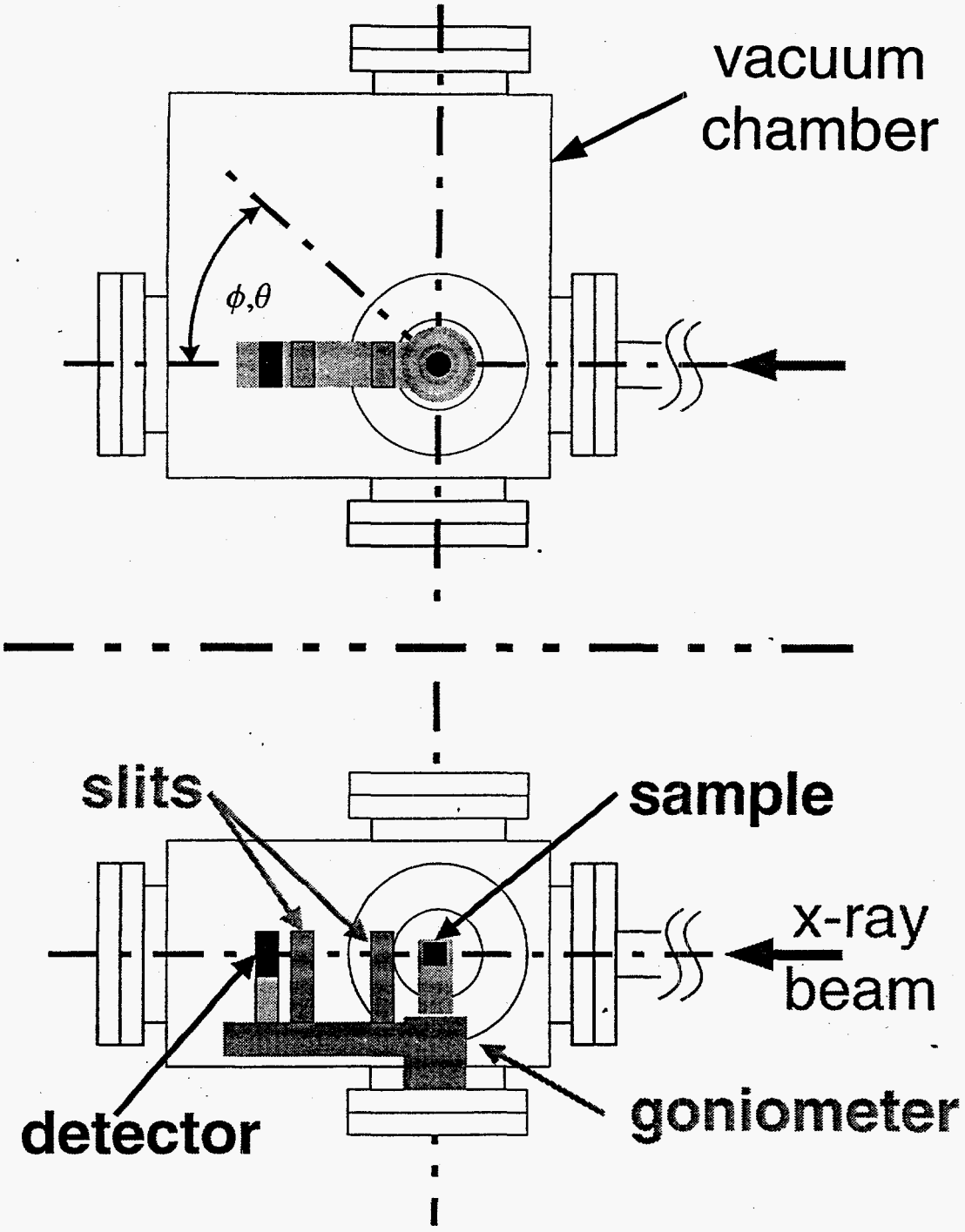

Figure 6 Schematic diagram of the UHV sample and detector chamber. For transmission and scattering studies, the detector is placed on a rotatable arm that also carries two slit assemblies located near the sample and detector respectively. The sample and detector can be rotated independently under computer control about a common axis through an angle (ϕ or θ respectively) that exceed $\pi/2$ radians. Although not shown in the figure, an appropriate detector, usually a solid state Ge or Si device, can be inserted through the port near the sample along an axis perpendicular to the direction of the incident x-ray beam, for fluorescence studies.

$$I(\lambda, x) = I_0(\lambda)\ e^{-a(\lambda)\,x/d}. \qquad \text{Equation 1}$$

Corresponding equations can be written for the left and right circularly polarized components of the radiation, hence characterizing the attenuation of left and right circularly polarized light by the quantities a_l and a_r respectively. The circular dichroism of a sample at some wavelength λ (or photon energy $h\nu$) can thus be represented by the equation

$$\Delta a_{CD} = a_l - a_r. \qquad \text{Equation 2}$$

If we presume that the incident intensity is independent of polarization, and define $\Delta I_{CD}(\lambda, d)$ as the difference in intensity of the two polarization states as the beam emerges from the sample, and $I(\lambda, d)$ as the average transmitted intensity *i.e.*,

$$\Delta I_{CD} = I_l - I_r \quad \text{and} \quad I = \tfrac{1}{2} I_l + \tfrac{1}{2} I_r, \qquad \text{Equation 3}$$

then to a first order approximation, the circular dichroism, Δa_{CD}, can be expressed in terms of the observable quantities I and ΔI_{CD} by the equation[1]

$$\Delta a_{CD} = -\ \Delta I_{CD} / I. \qquad \text{Equation 4}$$

This result implies that measurement of circular dichroism requires detection of only the beam transmitted by a sample. No knowledge of the intensity of the incident beam is required for transmission-detected circular dichroism. Circular dichroism can also be detected by monitoring the fluorescence generated by a sample, but the relationship between the circular dichroism of the sample and observable intensities of fluorescence is somewhat more complicated.[20]

The absorption spectrum of a sample is a plot $a(\lambda)$, defined by the equation

$$a(\lambda) = ln[I_0(\lambda)/I(\lambda)] \qquad \text{Equation 5}$$

where I_0 is the intensity recorded by the detector at wavelength λ in the absence of a sample, provided that the intensity of the source is constant in time between the measurement of I and I_0. In the case of synchrotron radiation, however, the incident intensity decays monotonically in time over the course of a "fill" of the storage ring. Recording the signal from a metal mesh detector located before the sample provides a measure of incident intensity that is used to normalize the observed values of the average intensity at the detector to correct for such variations in incident intensity. Note that such normalization is not required for the detection of circular dichroism .

2.7 Double Synchronous Detection of Circular Dichroism

The use of a chopper to block switching transients from reaching the detector leads to a simple but sensitive method for measuring transmission-detected circular dichroism. Switching transients occur twice during each cycle of the elliptically polarizing wiggler: first on the left-to-right transition and then on the right-to-left transition, as shown in Figure 4. Thus, the chopper must be operated at twice the frequency of the wiggler, as shown schematically in Figure 3. A phase-sensitive detector (*i.e.*, "lock-in" amplifier") connected to the output of the transmission

[1] This equation holds provided that $\Delta A_{CD} \ll I$. The As are extrinsic parameters. Corresponding intrinsic parameters can be used in their place by normalizing by the optical path length, d and/or the concentration of the absorbing species. Correction must also be made for the fact that the elliptically polarizing wiggler does not produce completely elliptically polarized radiation.

detector and tuned to the frequency of the wiggler, f, will record a signal proportional to the differences in intensities reaching the detector for the two polarization states, *i.e.*, ΔI. A second lock-in also connected to the detector output but tuned to $2f$, *i.e.*, the same frequency as the chopper, will detect the average intensity reaching the detector, *i.e.*, I. These relationships are illustrated in Figure 5. The use of two lock-in amplifiers eliminates the effects of any "zero-offset" or noise that may appear in the signal from the detector.

2.8 Computer System for Beamline Control and Data Acquisition

The beamline is controlled and data are acquired by a computer based on a Pentium processor (Intel, Santa Clara, CA) and NT operating system (Microsoft Corp, Redmond, WA). The computer controls the monochromator grating and exit-slit positions *via* a serial link to a modular stepping motor controller (Mclennan Servo Supplies, Ltd., Surrey, UK) that sends stepping pulses to the motors that move the grating and exit slit and returns data from their respective encoders. The goniometer that rotates the sample and the detector arm is programmed *via* a General Purpose Interface Bus (GPIB, IEEE–488) by a custom built stepping-motor controller.[21,22] The two lock-in amplifiers (7220 DSP, EGG Instruments Princeton, NJ) and chopper also are connected to the computer by the GPIB. Other analog signals, such as the output of a mesh detector located between the exit slit and the sample chamber, which monitors the intensity of the incident beam, are digitized and transmitted to the computer *via* auxiliary analog-to-digital converters that are part of the lock-in amplifiers. The computer–GPIB interface is a model PCI-GPIB (National Instruments, Austin, TX). Beamline control and data-acquisition programs are written in the Visual-Basic language (Microsoft Corp., *ibid*). Data can be transferred over a high speed network and stored on a remote server using the data-system protocol described elsewhere.[23]

3. ACKNOWLEDGMENTS

Research supported by the Office of Biological and Environmental Research and the Office of Basic Energy Sciences, United States Department of Energy

4. REFERENCES

1 M. Grosjean and M. Legrand, "Polarimetrie. - Appareil de mesure du dichroïsme circulaire dans le visible et l'ultraviolet," Compt. Rend. **251**, 2150-2153, 1960.

2 J. C. Kemp, "Piezo-optical birefringence modulators: new use for a long-known effect," Journal of the Optical Society of America **59**, 950-954, 1969.

3 L. F. Mollenauer, D. Downie, H. Engstrom, and W. B. Grant, "Stress plate optical modulator for circular dichroism measurements," Applied Optics **8**, 661-665, 1969.

4 S. N. Jasperson and S. E. Schnatterly, "An improved method for high reflectivity ellipsometry based on a new polarization modulation technique," Review of Scientific Instruments **40**, 761-767, 1969.

5 T. A. Keiderling, "Vibrational circular dichroism: Applications to conformational analysis of biomolecules," in *Circular Dichroism and the Conformational Analysis of Biomolecules*, edited by Gerald D. Fasman (Plenum Press, New York, 1996), pp. 555-598.

6 J. C. Sutherland, "Circular dichroism using synchrotron radiation: from ultraviolet to x-rays," in *Circular Dichroism and the Conformational Analysis of Biomolecules*, edited by Gerald D. Fasman (Plenum Press, New York, 1996), pp. 599-633.

7 U. Heinzmann, "Experimental determination of the phase differences of continuum wavefunctions describing the photoionisation process of xenon atoms I. Measurement of the spin polarisations of photoelectrons and their comparison with theoretical results," Journal of Physics B: Atomic and Molecular Physics **13**, 4353-4366, 1980.

8 U. Heinzmann, B. Osterheld, and F. Schafers, "Measurement and calculations of the circular polariation and of the absolute intensity of synchrotron radiation in the wavelength range from 40 to 100 nm," Nuclear Instruments and Methods **195**, 395-398, 1982.

9 B. Holmquist, "The Magnetic Optical Activity of Hemoproteins," in *The Porphyrins*, edited by David Dolphin (Academic Press, New York, 1978), Vol. **III**, pp. 249-270.

10 J. C. Sutherland and B. Holmquist, "Magnetic Circular Dichroism of Biological Molecules," Annual Review of Biophysics and Bioengineering **9**, 293-326, 1980.

11 J. van Elp, S. J. George, J. Chen *et al.*, "Soft x-ray magnetic circular dichroism: A probe for studying paramagnetic bioinorganic systems," Proc. Natl. Acad. Sci. U. S. A. **90**, 9664-9667, 1993.

12 G. D. Fasman, "Circular dichroism and the conformational analysis of biomolecules," (Plenum Press, New York, 1996).

13 L. Alagna, S. Di Fonzo, T. Prosperi, S. Turchini, P. Lazzeretti, M. Malagoli, R. Zanasi, C. R. Natoli, and P. J. Stephens, "Random phase approximation calculations of K-edge rotational strengths of chiral molecules: propylene oxide," Chemical Physics Letters **223**, 402-410, 1994.

14 A. Friedman, X. Zhang, S. Krinsky, E. Blum, and K. Halbach, "Polarized wiggler for NSLS x-ray ring," presented at the 1993 Particle Accelerator Conference, Washington D.C., 1993 (unpublished).

15 A. Friedman, S. Krinsky, and E. Blum, Report No. BNL-47317, 1992.

16 E. Gluskin, D. Frachon, P. M. Ivanov *et al.*, "The elliptical multipole wiggler project," presented at the 1995 IEEE Particle Accelerator Conference, Dallas, Texas, USA, 1996 (unpublished).

17 M. R. Howells, "Gratings and monochromators," in *Center for x-ray optics x-ray data booklet*, edited by D. Vaughn (Lawrence Berkeley Laboratory, Berkeley, CA, 1986), pp. 5/25-25/32.

18 H. Winick, "Synchrotron Radiation Sources, A Primer," (World Scientific Publishing Company, Inc., River Edge, New Jersey, 1994).

19 J. C. Sutherland, G. D. Cimino, and E. J. Desmond, "Simultaneous Measurement of Fluorescence and Phosphorescence Using Synchronously Gated Photon Counters," Analytical Biochemistry **97**, 158-165, 1979.

20 J. C. Sutherland, G. D. Cimino, and J. T. Lowe, "Magnetic circularly polarized fluorescence of tetraphenylporphine," in *Excited States of Biological Molecules* (John Wiley and Sons, New York, 1976).

21 S. K. Feng-Berman and D. P. Siddons, Report No. BNL-48962, 1993.

22 S. K. Feng-Berman, D. P. Siddons, and L. Berman, "National Synchrotron Light Source Beam Line Data Acquisition and Analysis Computer System," Nuclear Instruments and Methods in Physics Research A **347**, 603-606, 1994.

23 J. C. Sutherland, D. C. Monteleone, and B. M. Sutherland, "Computer Network for Data Acquisition, Storage, and Analysis," Journal of Photochemistry and Photobiology, B **40**, 14-22, 1997.